"Quasi-freestanding" Graphene-on-Single Walled Carbon Nanotube Electrode for Applications in Organic Light-emitting Diode

Yanpeng Liu, Eun Jung, Yu Wang, Yi Zheng, Eun Ji Park, Sung Min Cho, and Kian Ping Loh**

An air-stable transparent conductive film with "quasi-freestanding" graphene supported on horizontal single walled carbon nanotubes (SWCNTs) arrays is fabricated. The sheet resistance of graphene films stacked via layer-by-layer transfer (LBL) on quartz, and modified by 1-Pyrenebutyric acid N-hydroxysuccinimide ester (PBASE), is reduced from 273 Ω/sq to about 76 Ω/sq. The electrical properties are stable to heat treatment (up to 200 °C) and ambient exposure. Organic light-emitting diodes (OLEDs) constructed of this carbon anode (T ≈ 89.13% at 550 nm) exhibit ≈88% power efficiency of OLEDs fabricated on an ITO anode (low turn on voltage ≈3.1 eV, high luminance up to ≈29 490 cd/m^2, current efficiency ≈14.7 cd/A). Most importantly, the entire graphene-on-SWCNT hybrid electrodes can be transferred onto plastic (PET) forming a highly-flexible OLED device, which continues to function without degradation in performance at bending angles >60°.

1. Introduction

Transparent conductive films (TCFs) have wide ranging applications in organic light-emitting diodes (OLEDs), solar cells, touch panels and other flexible electronics. Currently, the high cost of indium and brittle nature of indium metal oxides (ITO) prevent its widespread adoption in applications that demand low cost and mechanical flexibility. Many efforts have been dedicated towards fabricating high performance and low cost TCFs. Among various materials, graphene films have become prime candidate with its outstanding mechanical strength, flexibility, transparency (T) and conductivity.[1–4] Due to its atomic thickness, graphene has to be supported on optically transparent substrates like quartz glass and poly(ethyleneterephthalate) (PET) when used as TCFs. However, charged impurity centers and optical phonon scattering due to the polar substrate reduces the intrinsic mobility of the carriers.[5,6] Recently, several research groups reported that metallic grid or metal nano-structure could enhance the performance of graphene films, affording a sheet resistance of ≈20 Ω per square (Ω/sq.) at 90% transmittance.[7,8] However, expensive metals (Ti, Ag and Au), high vacuum sputter system or photolithography are indispensable to fabricate the metal grid, which increase the economic footprint of the system. Several research groups reported low sheet resistance of multilayer graphene via layer by layer transfer and doping.[9–11] After p-doping with HNO_3 or $AuCl_3$, the sheet resistances of 4-layered graphene films are reduced by about 38% and 61% (87 Ω/sq. undoped; 54 Ω/sq. HNO_3 doped; 34 Ω/sq. $AuCl_3$ doped), respectively. Using p-doped

Y. P. Liu,[+] Dr. Y. Wang, Dr. Y. Zheng, Prof. K. P. Loh
Department of Chemistry
National University of Singapore
3 Science Drive 3, 117543, Singapore
E-mail: chmlohkp@nus.edu.sg
E. Jung,[+] E. J. Park, Prof. S. M. Cho
School of Chemical Engineering
Sungkyunkwan University (SKKU)
Suwon, Gyeonggi, 440–746, Korea
E-mail: sungmcho@skku.edu
[+]These authors contributed equally to this work.

DOI: 10.1002/smll.201301829

NANO MICRO small

4-layer graphene as electrode, Ahn and coworkers achieved high power efficiency for OLEDs (PE, 102.7 lm/W for graphene anode and 85.6 lm/W for ITO reference, lm = luminous flux).[11] However, the drawbacks were pointed out: 1) $AuCl_3$ will dramatically increase the roughness of the film; 2) HNO_3 acid doping is not stable and the effect decays with time. Therefore, there is a need to identify a robust method to improve the sheet conductivity of CVD graphene whilst keeping good optical transparency. In this work, we fabricated an air-stable TCFs with "quasi-freestanding" graphene supported on horizontal single walled carbon nanotubes (SWCNTs) arrays. The sheet resistance of graphene films stacked via layer-by-layer transfer (LBL) on quartz, and modified by 1-Pyrenebutyric acid N-hydroxysuccinimide ester (PBASE), was reduced from 273 Ω/sq to about 76 Ω/sq. The electrical properties are stable to heat treatment (below 200 ºC) and ambient exposure. By engineering the PIN (an intrinsic emission layer sandwiched in between p- and n-doped transport layers) junction, OLEDs constructed of this carbon anode (CNT/PBASE/FLG/PBASE/FLG/PBASE, T≈89.13% at 550 nm) exhibit ≈88% power efficiency of OLEDs fabricated on ITO anode (low turn on voltage ≈ 3.1 eV, high luminance up to ≈29 490 cd/m^2 (best up to date), current efficiency ≈14.7 cd/A). With further optimization of the OLEDs structure and materials, it should have the potential to reach >80 lm/W power efficiency.

2. Results and Discussion

To fabricate well aligned SWCNTs arrays over a large area, inkjet printer was used to directly write catalyst patterns for SWCNTs growth. 5 mM cobalt chlorides ($CoCl_2$)/polyvinylpyrrolidone (PVP) in ethanol were printed onto ST-cut single crystal quartz substrate and these serve as the catalysts for the CNT growth, as shown in **Figure 1**a. Well aligned SWCNTs

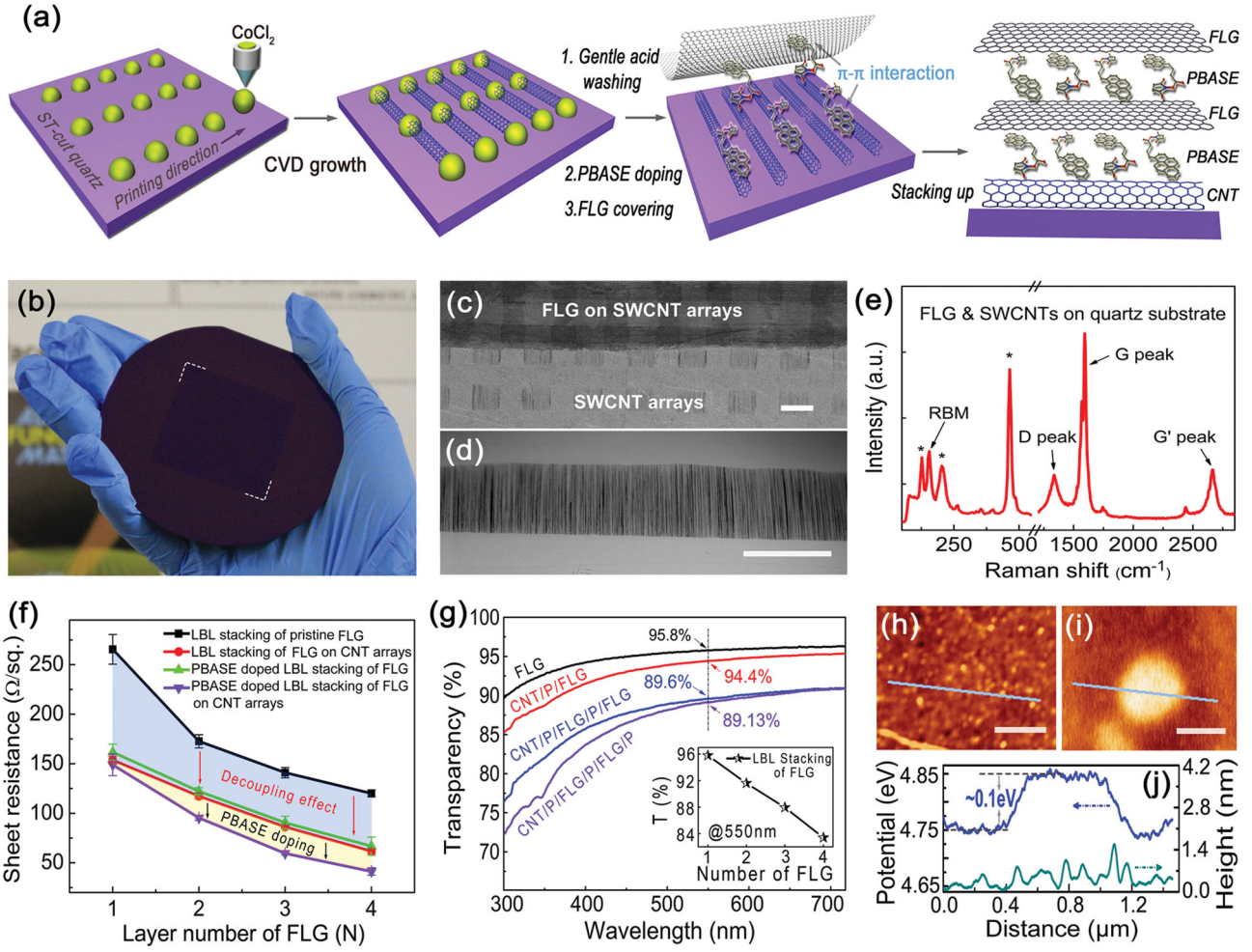

Figure 1. a) Schematic diagram of the fabrication route for full carbon TCFs. First, ink-jet printer was employed to pattern catalyst on quartz substrates for the CVD growth of SWNTs arrays. Full carbon TCFs (SWCNT/PBASE/FLG/PBASE/FLG/PBASE) are assembled in a layer by layer fashion. b) Optical image of the large-area TCFs; SEM images of c) FLG on top of horizontal SWCNTs grids on quartz. d) well-aligned SWCNT arrays grown on single crystal quartz using ink-jet printed catalyst. e) Raman spectrum of FLG and SWCNTs arrays (peaks with * are due to quartz substrate). f) Sheet resistance of as-prepared TCFs via SWCNT decoupling, followed by PBASE modification for different FLGs. g) Transparency of CNT, PBASE modified and layer-dependent TCFs (insert graph: UV-vis spectrum of various number of as-synthesized FLG on quartz in the visible light wavelength range), P indicate PBASE. h) Topography and i) surface potential image of PBASE-modified FLG on silicon wafer. j) Work function and topographical profiles of bare FLG and PBASE-modified FLG.

arrays were successfully grown on these by the standard CVD process using quartz tube furnace. Depending on various catalysts designs and precise growth time controlling, sundry SWCNTs patterns (Figure S1a,b) could be achieved. Atomic force microscopy (AFM) images (Figure S1d,e) show that these SWCNTs have diameters that vary from 0.8 to 1.8 nm. By means of PMMA mediator, the SWCNT arrays can be peeled off from quartz substrates and loaded onto the target substrates with nearly perfect alignment.[12]

At the same time, high quality, few-layer graphene (FLG) was grown using ethanol as the carbon precursor by low pressure chemical vapor deposition (as described in the Supporting Information). After CVD growth, graphene films were transferred onto the pre-grown SWCNTs arrays with the assistance of a PMMA supporting layer.[13] Raman spectroscopy, AFM and transmission electron microscopy (TEM) (Figure S2 and S3) results reveal that the as-grown graphene film is bilayer over large area (coverage > 99%). To engineer the surface energy and improve the electrical conductivity, the graphene films were immersed in 5 mM PBASE in dimethylformaldehyde (DMF) solution for 8 h at 80 °C to allow the PBASE molecules to adsorb by π–π interactions.[14,15] After drying, another CVD-grown FLG layer was directly stacked onto the first FLG-on-SWCNT array sample, this has the effect of further reducing the sheet resistance.

Figure 1b shows the optical image of the FLG film supported on a 4-inch wafer. Figure 1c,d shows the scanning electron micrographs of the hybrid graphene-SWCNT films. From these images, the FLG film and SWCNTs grids maintain their distinct morphologies. Raman measurement was performed to characterize the full carbon TCFs on quartz (Figure 1e). Compared with Raman data of the FLG in Figure S2a, the spectrum clearly shows additional peaks between 140 and 220 cm^{-1}, which are assignable to the radical breathing mode (RBM) of SWCNTs.[16,17] As shown in **Figure 2**f, the sheet resistance of the first layer of FLG film reduces from 265 to 154 Ω/sq after mounting it on the SWCNT grid, with only a very slight decrease in the total transmittance (≈0.93%, Figure 1g). After adding a second layer of FLG and with PBASE modification, the sheet resistance further decreases to ≈ 90 Ω/sq (Figure 1f, purple line). The transparency at this stage is about 89% at 550 nm (Figure 1g). Scanning Kelvin probe microscope (SKPM) was applied to investigate the surface potential change by PBASE.[18] Figure 1h,i display the topographical and surface potential image of PBASE modified FLG placed on silicon wafer with 300 nm SiO_2. The PBASE adlayer, distinguished by ≈0.35 nm height difference, increases the work function of the FLG surface by 0.1 eV in atmosphere.[15,19]

From the SEM image of Figure 2a, it is clear that there is a color contrast (highlighted in red) between the FLG with and without the SWCNTs scaffold beneath. The aligned SWCNTs effectively decoupled the FLG from the substrate and no obvious ripples or cracking of upper FLG layer was observed. To evaluate chemical and thermal stability, samples with the structure (CNT/PBASE/FLG/PBASE/FLG/PBASE) were exposed to the ambient (Figure 2c) or placed in the hot oven (inset in Figure 2c). Following air exposure, the sheet resistance of the TCFs decreases from 105 Ω/sq to 76 Ω/sq after the first week due to relaxation of the strained film and remains constant thereafter.[7,13] Thermal stress test in hot oven shows that the hybrid TCFs can be heated to 200 °C (limited by the oven) without degradation in electrical conductivity and transparency.

In view of its low sheet resistance and high transparency, the graphene-CNT hybrid films with the hierachically stacked structure of (SWCNT/PBASE/FLG/PBASE/FLG/PBASE) were used as anodes in small molecule phosphorescent OLEDs with the PIN structure. The control device was fabrciated using ITO. The basic architecture of our OLEDs is

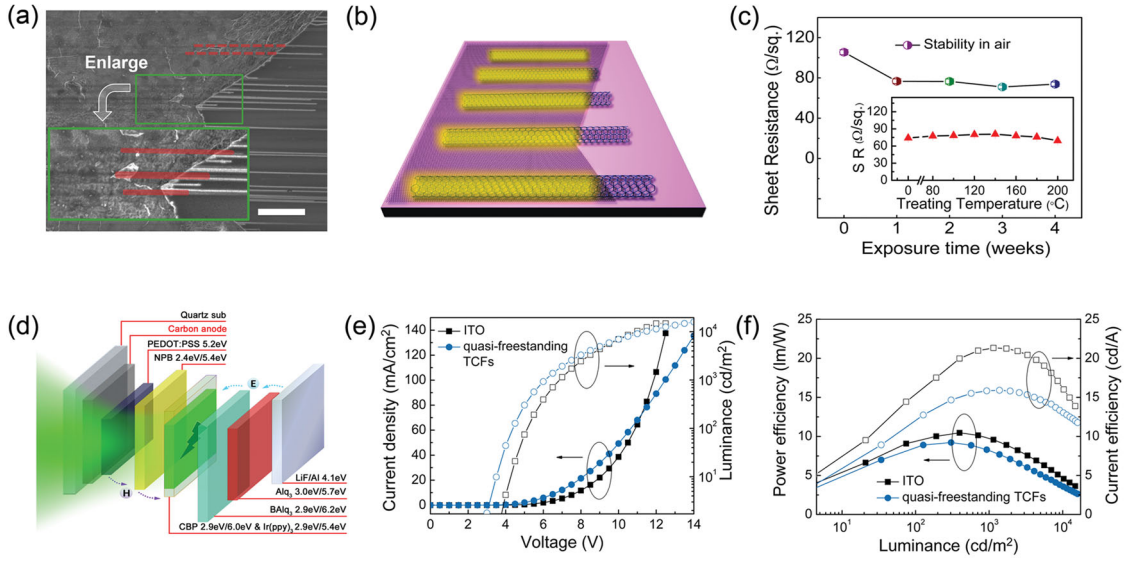

Figure 2. a) SEM image of FLG on SWCNT arrays, scale bar is 5 µm. b) Schematic diagram of "quasi-freestanding" FLG-on-SWCBT TCFs electrode. c) Stability test of TCFs in air and when subjected to high temperature (inserted graph). d) A schematic drawing of OLEDs structure. e), f) Luminance-Voltage–current density and current efficiency–luminance–power efficiency characteristics of devices using ITO and full carbon TCFs, respectively. The maximum current efficiencies are taken at the point with maximum power efficiency.

NANO MICRO small

composed of five layers: a hole-injecting PEDOT:PSS (poly(3, 4-ethylenedioxythiophene)/poly(styrene), with and without a perfluorinated ionomer (PFI)) layer, a hole-transporting NPB(N,N′-bis(naphthalen-1-yl)-N,N′-bis(phenyl) benzidine) layer, an emissive CBP (4,4′-N,N′-dicarbazolylbiphenyl))-doped with a phosphorescent dopant $Ir(ppy)_3$ (tris(2-phenylpyridine) iridium(III)) layer, a hole-blocking $BAlq_3$ (bis(2-methyl-8-quinolinolato-N1,O8)-(1,10-biphenyl-4-olato) aluminum) layer, an electron-transporting Alq_3 (tris(8-hydroxyquionline) aluminum) layer, and an aluminum cathode (Al/LiF) layer, as depicted in Figure 2d. With this layer sequence, the highest occupied molecular orbitals (HOMO) on the hole transporting side are well aligned and the hole injection barrier is reduced, and vice versa on the electron transporting side. After optimizing each layer, we measured the performance of the OLED on ITO and our hybrid FLG-on-SWCNT anodes and compared the luminance (cd/m^2), current efficiency (CE, cd/A) and power efficiency (PE, lm/W).

As shown in Figure 2e and f, the luminance of our carbon-based devices can easily reach >10,000 cd/m^2 (highest ≈29,490 cd/m^2 at 351.1 mA/cm^2) at low current density (73.1 mA/cm^2, Figure 2e). The luminance value has increased by several orders of magnitude compared to previously reported results using graphene anodes and green emitter.[20,21] The green OLEDs based on FLG-on-SWCNT anode has a lower turn-on voltage (≈3.1 V) than bare ITO (≈3.55 V), which is aided by its higher work function. Moreover, the current efficiency and power efficiency (**Figure 3**f, 9.2 lm/W and 14.7 cd/A at 300 cd/m^2) are comparable to ITO anode (PE:10.46 lm/W; CE:19.97 cd/A at 396.2 cd/m^2) and much higher than previous reports using graphene, even though this value is still far from the best performing device (102.7 lm/W and 91.8 cd/A).[11,20,21] We believe that the OLEDs fabricated using our methods should be able to achieve PE > 80 lm/W after further optimization.

In order to verify the importance of hierarchical stacking of the various components on performance parameters like

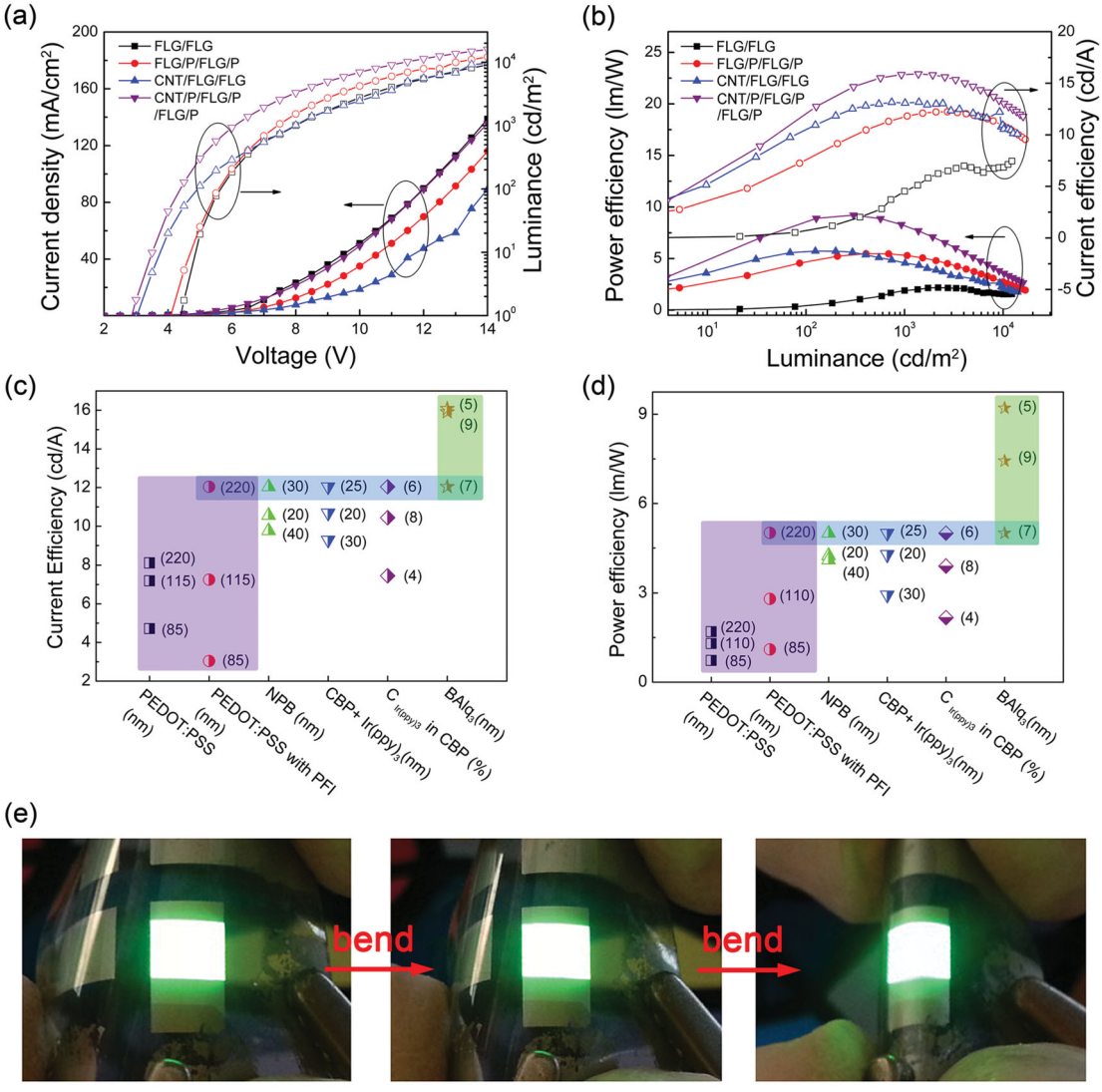

Figure 3. Performances of green OLED using hierarchically stacked full-carbon TCFs as anodes in green OLEDs a) and b) luminance–voltage–current density and current efficiency–luminance–power efficiency characteristics of devices with various full carbon TCFs. c) and d) CE and PE dependence on each function layer. e) Flexiblity test at various bending angles.

power efficiency and current efficiency, different combinations of FLG, SWCNTs arrays and PBASE doping were tested. These include the pristine FLG graphene stack (FLG/FLG), two FLG layers on SWCNT arrays (CNT/FLG/FLG), two FLG layers with PBASE modification of each layer (FLG/PBASE/FLG/PBASE) and two FLG layers on SWCNT arrays with PBASE modification of each layer (CNT/PBASE/FLG/PBASE/FLG/PBASE), similar to Figure 1a. The current density-voltage-luminance plot and PE-luminance-CE plot of the four devices are shown in Figure 3a,b. OLEDs fabricated with stacks which have higher work function (FLG/PBASE/FLG/PBASE) and lower sheet resistance (CNT/FLG/FLG) have a lower turn on voltage (≈4.1 eV and ≈2.8 eV, respectively), higher PE (5.48 lm/W and 5.72 lm/W, respectively) and higher CE (12.23 cd/A and 13.15 cd/A, respectively) than those with higher transparency (FLG/FLG, ≈4.3 eV, 2.5 lm/W, and 7 cd/A). The PE and CE of OLEDs on CNT/PBASE/FLG/PBASE/FLG/PBASE show the best performance among all the combinations, despite of its lowest transparency of 89%. These results illustrate that the sheet resistance and work function are more critical performanc bottlenecks than transparency at >89% transparency.

In order to achieve high efficiency OLEDs, a balanced injection of holes and electrons into the emitting layer is important. For a fixed OLED structure and material composition, the most convenient way is to vary the thickness of all layers and change the dopant concentration of the emitting layer. The spots in blue region (Figure 3c and d) were chosen as the standard condition for univariate test. When graphene is used as the anode, the hole injection from graphene (work function is ≈4.6–4.75 eV) to NPB (work function is ≈5.4 eV) is unfavorable due to the large injection barrier (≈0.8 eV). In spite of this drawback, our FLG-on-SWCNT TCFs show CE ≈8.11 cd/A and PE ≈1.70 lm/W (Figure 3c and d, the purple zone), several times better than previously reported values.[20,21] The use of PFI (a tetrafluoroethylene-perfluoro-3,6-dioxa-4-methyl-7-octenesulphonic acid copolymer) increases the work function of PEDOT:PSS (to 5.95 eV) and enhances the hole injection from the TCFs to the hole transporting layer and hence improves the efficiency dramatically (red spot in the purple zone).[11,22] Thicker hole injection layer (HIL) can effectively cover the underlying anode and reduce the surface roughness of the FLG-on-SWCNT TCFs. As a result, higher CE (12.04 cd/A) and PE (5.01 lm/W) can be obtained using 220 nm HIL (spin speed: 1000 rpm). Finally, controlling the thickness of hole blocking layer (HBL) is important to achieve high efficiency after the hole injection problem is solved. However, Alq_3 usually shows very low electron mobility. If higher electron mobility materials were employed, the total power efficiency may easily reach ≈80 lm/W. Finally, the flexibility of the device was tested with various bending angles (Figure 3e). The working area continues to emit uniform green light at bent angles up to 90° and even after hundreds of bending cycles, which demonstrate that the FLG-on-SWCNT TCFs are suitable for flexible electronics.

3. Conclusion

In conclusion, we have fabricated transparent, highly conducting, "quasi-freestanding" graphene films supported on SWCNT arrays for applications as electrode in green OLEDs. Three key steps allow us to reduce the sheet resistance significantly and improve the film fabrication process. First, CVD growth using ethanol as the carbon precursor allows us to deposit predominantly bilayer graphene films which can be stacked hierarchically together to form a four-layer film. This is an improvement in process throughput compared to previous layer-by-layer stacking and doping needed for monolayer films. Second, due to substrate-decoupling effect by SWCNT arrays, the sheet resistance of the FLG on quartz is decreased nearly by half, with minimal reduction in transparency. Finally, surface treatment with PBASE increases the work function and further reduces sheet resistance. A typical FLG-on-SWCNT anode has transmission of ≈89% and sheet resistance of ≈76 Ω/sq. The green OLEDs fabricated from these exhibit low turn on voltage, high luminance, outstanding current efficiency (14.7 cd/A) and power efficiency (9.21 lm/W), which is comparable with the OLEDs device employing ITO anode with the same receipt. The efficiency can be improved further if more sophisticated OLEDs structures and materials are used. At present, this work demonstrates the premise of fabricating a highly stable (thermal and air-exposure) hybrid CNT-graphene electrode with robust electrical properties and high flexibility.

4. Experimental Section

CVD Growth of Graphene via Ethanol Precursor: Graphene films were produced in a thermal CVD furnace on copper foil using ethanol as the precursor by LP-CVD, similar to the previous methane-based CVD methods (see supporting information).[2–4]

CVD Growth of Horizontal SWCNT Arrays: In our experiments, SWCNT arrays are grown in a typical thermal tube furnace with cobalt chlorides ($CoCl_2$) as catalyst on ST-cut single crystal quartz substrates (see also supporting information).

Fabrication of OLED Devices: Please refer to the Supporting Information for the fabrication and measurements.

Supporting Information

Supporting Information is available from the Wiley Online Library or from the author.

Acknowledgements

K. P. Loh acknowledges funding support from MOE Tier 2 grant "Interface engineering of graphene hybrids for energy conversion" R-143–000–488–112.

[1] P. Matyba, H. Yamaguchi, G. Eda, M. Chhowalla, L. Edman, N. D. Robinson, *ACS Nano* **2010**, *4*, 637.
[2] K. S. Kim, Y. Zhao, H. Jang, S. Y. Lee, J. M. Kim, K. S. Kim, J.-H. Ahn, P. Kim, J.-Y. Choi, B. H. Hong, *Nature* **2009**, *457*, 706.
[3] X. S. Li, W. W. Cai, J. H. An, S. Kim, J. Nah, D. X. Yang, R. Piner, A. Velamakanni, I. Jung, E. Tutuc, S. K. Banerjee, L. Colombo, R. S. Ruoff, *Science* **2009**, *324*, 1312.
[4] Y. Wang, S. W. Tong, X. F. Xu, B. Özyilmaz, K. P. Loh, *Adv. Mater.* **2011**, *23*, 1514.
[5] X. Du, I. Skachko, A. Barker, E. Y. Andrei, *Nat. Nanotechnol.* **2008**, *3*, 491.
[6] E. H. Hwang, S. Adam, S. D. Sarma, *Phys. Rev. Lett.* **2007**, *98*, 186806.
[7] Y. Zhu, Z. Sun, Z. Yan, Z. Jin, J. M. Tour, *ACS Nano* **2011**, *5*, 6472.
[8] I. N. Kholmanov, C. W. Magnuson, A. E. Aliev, H. Li, B. Zhang, J. W. Suk, L. L. Zhang, E. Peng, S. H. Mousavi, A. B. Khanikaev, R. Piner, G. Shvets, R. S. Roff, *Nano Lett.* **2012**, *12*, 5679.
[9] F. Günes, H.-J. Shin, C. Biswas, G. H. Han, E. S. Kim, S. J. Chae, J.-Y. Choi, Y. H. Lee, *ACS Nano* **2010**, *4*, 4595.
[10] S. Bae, H. Kim, Y. Lee, X. Xu, J.-S. Park, Y. Zheng, J. Balakrishnan, T. Lei, H. R. Kim, Y. I. Song, Y.-J. Kim, K. S. Kim, B. Özyilmaz, J.-H. Ahn, B. H. Hong, S. Iijima, *Nat. Nanotechnol.* **2010**, *5*, 574.
[11] T. H. Han, Y. Lee, M. R. Choi, S. H. Woo, S. H. Bae, B. H. Hong, J. H. Ahn, T. W. Lee, *Nat. Photonics* **2012**, *6*, 105.
[12] L. Y. Jiao, B. Fan, X. J. Xian, Z. Y. Wu, J. Zhang, Z. F. Liu, *J. Am. Chem. Soc.* **2008**, *130*, 12612.
[13] X. S. Li, Y. W. Zhu, W. W. Cai, M. Borysiak, B. Y. Han, D. Chen, R. D. Piner, L. Colombo, R. S. Ruoff, *Nano Lett.* **2009**, *9*, 4359.
[14] R. J. Chen, Y. Zhang, D. Wang, H. Dai, *J. Am. Chem. Soc.* **2001**, *123*, 3838.
[15] Y. Wang, X. H. Chen, Y. L. Zhong, F. R. Zhu, K. P. Loh, *Appl. Phys. Lett.* **2009**, *95*, 063302.
[16] H. Kuzmany, W. Plank, M. Hulman, Ch. Kramberger, A. Gruneis, Th. Pichler, H. Peterlik, H. Kataura, Y. Achiba, *Eur. Phys. J. B.* **2001**, *22*, 307.
[17] L. Alvarez, A. Righi, T. Guillard, S. Rols, E. Anglaret, D. Laplaze, J. L. Sauvajol, *Chem. Phys. Lett.* **2000**, *316*, 186.
[18] Y. J. Yu, Y. Zhao, S. Ryu, L. E. Brus, K. S. Kim, P. Kim, *Nano Lett.* **2009**, *9*, 3430.
[19] X. S. Li, C. W. Magnuson, A. Venugopal, R. M. Tromp, J. B. Hannon, E. M. Vogel, L. Colombo, R. S. Ruoff, *J. Am. Chem. Soc.* **2011**, *133*, 2816.
[20] T. Sun, Z. L. Wang, Z. J. Shi, G. Z. Ran, W. J. Xu, Z. Y. Wang, Z. Y. Li, L. Dai, G. G. Qin, *Appl. Phys. Lett.* **2010**, *96*, 133301.
[21] H. Meng, Y. Dai, Y. Ye, J. X. Luo, Z. J. Shi, L. Dai, G. G. Qin, *J. Phys. D: Appl. Phys.* **2012**, *45*, 245103.
[22] T. H. Han, M. R. Choi, S. H. Woo, S. Y. Min, C. L. Lee, T. W. Lee, *Adv. Mater.* **2012**, *24*, 1487.

Received: June 13, 2013
Revised: August 25, 2013
Published online: October 29, 2013